

Resource-Efficient Digitized Adiabatic Quantum Factorization

Felip Pellicer

Universidad Internacional Menéndez Pelayo, 28040 Madrid, Spain

E-mail: fpellicer.q@proton.me

Juan José García-Ripoll

Instituto de Física Fundamental, IFF-CSIC, Calle Serrano 113b, 28006 Madrid, Spain

E-mail: jj.garcia.ripoll@csic.es

Alan C. Santos*

Instituto de Física Fundamental, IFF-CSIC, Calle Serrano 113b, 28006 Madrid, Spain

E-mail: ac.santos@iff.csic.es

*Author to whom any correspondence should be addressed

Abstract. Digitized adiabatic quantum factorization is a hybrid algorithm that exploits the advantage of digitized quantum computers to implement efficient adiabatic algorithms for factorization through gate decompositions of analog evolutions. In this paper, we harness the flexibility of digitized computers to derive a digitized adiabatic algorithm able to reduce the gate-demanding costs of implementing factorization. To this end, we propose a new approach for adiabatic factorization by encoding the solution of the problem in the kernel subspace of the problem Hamiltonian, instead of using ground-state encoding considered in the standard adiabatic factorization proposed by Peng *et al.* [1]. Our encoding enables the design of adiabatic factorization algorithms belonging to the class of *Quadratic Unconstrained Binary Optimization* (QUBO) methods, instead the *Polynomial Unconstrained Binary Optimization* (PUBO) used by standard adiabatic factorization. We illustrate the performance of our QUBO algorithm by implementing the factorization of integers N up to 8 bits. The results demonstrate a substantial improvement over the PUBO formulation, both in terms of reduced circuit complexity and increased fidelity in identifying the correct solution.

1. Introduction

Digitized Adiabatic Quantum Computing is a promising approach to solve optimization problems by implementing time-continuous adiabatic algorithms with gate-based quantum devices [2]. This hybrid model harnesses benefits from adiabatic formulation of quantum algorithms, which allows us to encode the solution of a given problem into the spectrum of a problem Hamiltonian [3, 4], and error-correction strategies of gate-based digitized quantum computation [5, 6, 7, 8]. The outcomes of this hybridization are digitized Variational Quantum Algorithms [9, 10]—such as QAOA [11]

and Variational Quantum Eigensolvers [12]—have emerged as flexible approaches to incorporate classical processing as crucial ingredient to enhance the efficiency of digitized computers for Noisy Intermediate-Scale Quantum Algorithms [13, 14, 15, 16, 17], and quantum simulations [18, 19, 20, 21, 22, 23].

Of particular interest to this work, digitized adiabatic protocols has been successfully applied to factorization problems [1, 24, 25, 26]. The digitized algorithm proposed in Ref. [1] harnesses the skills of QAOA in tracking the ground state of an adiabatic problem Hamiltonian for factorization belonging to the class of *Polynomial Unconstrained Binary Optimization* (PUBO). As shown in Ref. [27], PUBO problems can be reduced to simpler QUBO formulations, which are more efficiently evaluated in the quantum computers. In fact, while QUBO formulations provide Hamiltonians with two-body interaction terms, PUBO requires quantum platforms with native k -body interactions [27], or the efficient decomposition of these k -body terms into two-qubit gates. However, this task involves additional variables and a polynomial reduction that is NP-hard, where even the simplest transformations demand the introduction of additional variables [28].

In this paper, we introduce a new QUBO formulation of the adiabatic factorization problem that does not require additional variables or NP-hard polynomial reductions. The central idea of our approach is that adiabatic quantum computation does not inherently require the system to be initialized in its ground state. Any energy level can serve as the starting point, provided that the evolution remains adiabatic and transitions to neighboring states are minimized. Building on this insight, we demonstrate that adiabatic factorization can be reformulated as the preparation of the zero-energy eigenstate of a QUBO formula, enabling the development of a novel gate-efficient QAOA algorithm circuit for factorization. Furthermore, by comparing our digitized QUBO-based factorization with the conventional PUBO approach, we show that the proposed model achieves substantially better performance. Also, we analyze the underlying reasons why our QUBO formulation outperforms its PUBO counterpart, which is mainly related to the density of states of the QUBO and PUBO Hamiltonians around the subspace of eigenstates encoding the solution of the adiabatic factorization.

2. Methods

2.1. Adiabatic Quantum Factorization

The hard instances of factorization involve separating a large integer number $N \in \mathbb{N}_{>0}$ as a product of two odd prime numbers $(q, p) \in \mathbb{N}_{>0}$ satisfying $N = p \times q$. This amounts to finding the zeros of a function

$$F(N, p', q') = N - (2p' + 1) \times (2q' + 1), \quad (1)$$

where $p = 2p' + 1$ and $q = 2q' + 1$. As shown by Peng et al. [1], this problem is solved by a quantum computer that prepares the ground state $|\Psi_{\text{sol}}\rangle$ of the problem Hamiltonian $\hat{H}_{\text{QP}} = F(N, p', q')^2$ defined using the observables $\hat{p} = \sum_{i=1}^{n_p} 2^{i-1} \hat{x}_i$ and $\hat{q} = \sum_{j=1}^{n_q} 2^{j-1} \hat{y}_j$

that reconstruct natural numbers from independent sets of qubits $\hat{x}_i, \hat{y}_j \in \{0, 1\}$ in a quantum register. In this formulation, the problem Hamiltonian is the polynomial

$$\hat{H}_{\text{QP}} = \left[N\mathbb{1} - \left(\sum_{\ell=1}^{n_p} 2^\ell \hat{x}_\ell + \mathbb{1} \right) \left(\sum_{m=1}^{n_q} 2^m \hat{y}_m + \mathbb{1} \right) \right]^2, \quad (2)$$

and the ground state is the set of bits that minimize the energy

$$|\Psi_{\text{sol}}\rangle = |p'\rangle \otimes |q'\rangle = (|x_1\rangle \otimes \cdots \otimes |x_{n_p}\rangle) \otimes (|y_1\rangle \otimes \cdots \otimes |y_{n_q}\rangle). \quad (3)$$

The largest number of qubits required to encode this problem are [1]

$$n_p = \mathcal{S}(\lfloor \sqrt{N} \rfloor_O) - 1, \quad n_q = \mathcal{S}\left(\left\lfloor \frac{N}{3} \right\rfloor\right) - 1, \quad (4)$$

where $\lfloor X \rfloor$ denotes the *largest integer* not larger than X , $\lfloor X \rfloor_O$ is the *largest odd integer* not larger than X , and $\mathcal{S}(X) \sim \lceil \log_2(X) \rceil$ is the *smallest number* of bits required for representing X .

The formulation of factoring as a ground state search means that this problem can be solved using adiabatic quantum computers, quantum annealers and any other adiabatic state preparation methods for digital quantum computers. Unfortunately, the Hamiltonian in Eq. (2) corresponds to a family of PUBO problems that involve non-local three- and four-qubit interactions $Z_3 = \hat{\sigma}_\ell^z \hat{\sigma}_m^z \hat{\sigma}_k^z$ and $Z_4 = \hat{\sigma}_\ell^z \hat{\sigma}_m^z \hat{\sigma}_k^z \hat{\sigma}_n^z$, gathering qubits from arbitrary locations in the quantum register. These non-local terms complicate the use of quantum annealers or other quantum optimizers, because they require establishing interactions among distant quantum objects—which may be impossible, depending on the architecture, or may require the use of multiple auxiliary qubits [29].

In digital applications, these non-local terms complicate the implementation of evolution with the Hamiltonian, $\exp(-i\hat{H}_{\text{QP}}\delta t)$, which requires two-, three- and four-partite controlled phases, $\exp(-iZ_3)$ or $\exp(-iZ_4)$, which must be decomposed into multiple applications of native two-qubit gates. For these reasons, PUBO-based digitized factorization has been limited to efficient (high fidelity) factorization achieved for numbers up to 91 [25]. For higher numbers, the success probability for factorization drastically decreases below 20% [18], even using machine learning techniques.

2.2. Null-subspace encoding and the QUBO Hamiltonian

Let us now discuss an alternative formulation of the factoring problem that addresses all the challenges discussed above. The key idea in our proposal is the realization that the adiabatic theorem equally applies to the preparation of ground state as to the creation of higher excited states—a fact demonstrated experimentally, for instance, in Ref. [23]. With this in mind, let us define a new factorization protocol as the preparation of the zero eigenstates $\hat{H}_{\text{LP}} |\Psi_{\text{sol}}\rangle = 0$ of a Hamiltonian defined as

$$\hat{H}_{\text{LP}} := F(N, \hat{p}', \hat{q}') = N\mathbb{1} - \left(\sum_{\ell=1}^{n_p} 2^\ell \hat{x}_\ell + \mathbb{1} \right) \left(\sum_{m=1}^{n_q} 2^m \hat{y}_m + \mathbb{1} \right), \quad (5)$$

This is a *linearized* alternative to the \hat{H}_{QP} introduced in Eq. (2). While the co-prime factors are defined by the same quantum eigenstates of both models, with $\langle \Psi_{\text{sol}} | \hat{H}_{\text{LP}} | \Psi_{\text{sol}} \rangle = \langle \Psi_{\text{sol}} | \hat{H}_{\text{QP}} | \Psi_{\text{sol}} \rangle = 0$, in \hat{H}_{LP} the solution is an excited state living in the *kernel subspace* of \hat{H}_{LP} . Most important, the problem Hamiltonian \hat{H}_{LP} is now a QUBO model that only contains two-body interactions. This makes the implementation more accessible for quantum simulators and digitized adiabatic protocols. Finally, and equally important, the eigenenergies of \hat{H}_{LP} in the computational basis are given by the values of the quadratic function $F(N, p', q')$ over all integer values of p' and q' . This spectrum grows more slowly, a fact that affects (positively) the instantaneous energy gaps and the performance of the adiabatic preparation protocols.

This simplified formulation is challenging for quantum computers and quantum simulators because it involves long-range interactions, and because the preparation of an excited state lifts all the protections against decoherence expected from an adiabatic quantum computing framework [30]. Nevertheless, the resulting model is still much simpler than the PUBO formulation and opens the door to efficient digitized approximations. In particular, this Hamiltonian is of comparable difficulty to other models used in variational quantum computation [31], and for that reason the following sections will explore variational QAOA protocols based on this new model.

2.3. Variational Algorithm for Adiabatic Factorization

Similarly to digitized adiabatic dynamics, variational algorithms are an efficient paradigm to simulate quantum annealing using gate-based quantum devices. Among the class of VQA, a way to connect quantum annealers and digital computers is provided by the QAOA [11, 13]. The algorithm aims to approximate the ground state of a cost Hamiltonian whose minimum encodes the optimal solution. At its core, QAOA applies the same strategy as AQC, driving the system from a easy-to-prepare ground state $|\psi_{\text{inp}}\rangle$ of the initial Hamiltonian \hat{H}_{ini} , to the output solution state $|\psi_{\text{sol}}\rangle$ enconded in the *ground state* of the problem Hamiltonian \hat{H}_{P} . To this end, QAOA constructs a parametrized quantum state (ansatz) by sequentially applying two alternating types of unitaries derived from these two main Hamiltonians. Using the QAOA terminology, the problem Hamiltonian \hat{H}_{P} is identified as the cost Hamiltonian, which encodes the objective function of the optimization problem. On the other hand, \hat{H}_{ini} is named mixing Hamiltonian \hat{H}_{M} , which introduces transitions between computational basis states to enable exploration of the solution space.

In the particular case of AQF, the QAOA algorithm starts with the initial state $|\psi_0\rangle = |+\rangle^{\otimes n}$, $|\pm\rangle = (|0\rangle \pm |1\rangle)/\sqrt{2}$, as it is a uniform superposition of all computational states of n bits. For this reason, the mixer Hamiltonian is defined as $H_{\text{M}} = \Omega \sum_{k=1}^n \hat{\sigma}_n^x$, guaranteeing that $|\psi_0\rangle$ is the ground state of the standard adiabatic protocol. On the other hand, in order to keep the same mixer Hamiltonian, the QUBO approach requires a different state initialization, as we need to start the evolution from the null-subspace of \hat{H}_{LP} . This is done by choosing $|\psi_0^{\text{LP}}\rangle = |+\rangle |-\rangle \cdots |+\rangle |-\rangle$. Similar to $|\psi_0\rangle$, $|\psi_0^{\text{LP}}\rangle$ also

represents a uniform superposition of all computational states. The only concern we need to take into account is the case in which the number of qubits n is not odd, as in this case the state $|\psi_0^{\text{LP}}\rangle$ is not the zero energy eigenstate of \hat{H}_{LP} . However, our QAOA algorithm is robust against this small deviation from the null-subspace of the QUBO Hamiltonian. Indeed, our QAOA algorithm performs efficiently even if we start both algorithms in state $|\psi_0\rangle$ [32], which is a disadvantageous scenario for \hat{H}_{LP} .

For the integration with classical optimizers, we employ cost functions defined in terms of the Hamiltonian that serves as the reference for constructing the QAOA circuit. Specifically, the PUBO-based circuit minimizes the cost function $\mathcal{C}_{\text{QP}} = \langle \hat{H}_{\text{QP}} \rangle$, whereas the QUBO-based approach relies on $\mathcal{C}_{\text{LP}} = \langle |\hat{H}_{\text{LP}}| \rangle$. The absolute value considered for the QUBO Hamiltonian guarantee that algorithm will find the desired state, with zero eigenvalue, through standard classical optimizers. Therefore, this enables that the optimization landscape of \mathcal{C}_{LP} is explored by the same classical algorithm employed for \mathcal{C}_{QP} , ensuring consistent performance evaluation across both methods. We also consider other strategies to define the cost function, which provides similar results [32].

3. Results and Discussions

In this section we present the main results of this work. We start by analyzing the performance of the PUBO and QUBO approaches for factorization of a 5-bits number. Then, we increase the complexity of the problem, factorizing up to 8-bits numbers. To end, we discuss about the mechanism behind the enhancement promoted by the QUBO Hamiltonian, leading to an intuitive explanation of why our proposal outperforms the PUBO Adiabatic QAOA model.

3.1. Factorizing the number 25

In order to demonstrate the enhancement promoted by our protocol, first let us to discuss its performance by factorizing small numbers. In particular, we consider the factorization of $N = 25$, which is a 5-bits number. To this, the adiabatic algorithm requires a minimum of 4 qubits, and the QAOA circuit is shown in Figs. 1a and 1b. The set of information in Fig. 1 is the first result of our work.

From Figs. 1a and 1b it is possible to identify the significant simplification of the QAOA circuit to implement the QUBO adiabatic Hamiltonian for the digitized algorithm, in comparison with the standard protocol. This enhancement become even more strong if we take into account that three-qubit and four-qubit operations in Figs. 1a need to be decomposed into two-qubit gates to be compared to Fig. 1b. As shown in Fig. 1c, taking as reference the decomposition of ZZ -interaction into CNOTs and local Z rotations, a n -body ZZ interaction needs $2n$ CNOTs.

This analysis shows that the 34-CNOTs circuit, per layer, required by the standard factorization is replaced by a 8-CNOTs circuit per layer, if we use the linear protocol. In addition, even most relevant, as shown in Figs. 1d and 1e, the QUBO algorithm

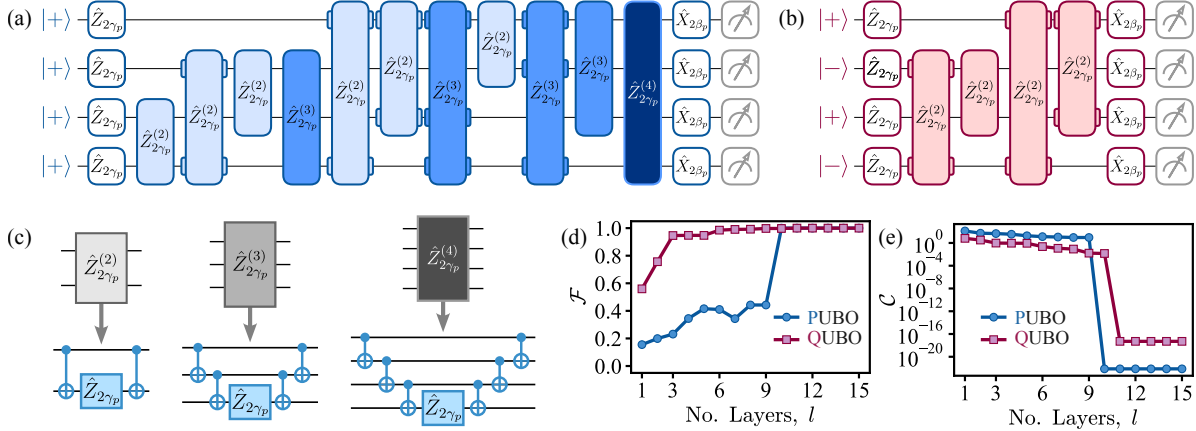


Figure 1. Single layer circuit of the (a) PUBO and (b) QUBO algorithms for factoring $N = 25$. While PUBO circuit requires three- and four-qubit gates, which can be decomposed according the circuits in (c), the QUBO algorithm requires two-qubit gates only. We define the circuit gates as $\hat{Z}_{2\gamma_p} = \exp(i\gamma_p \hat{\sigma}_k^z)$, $\hat{X}_{2\beta_p} = \exp(i\beta_p \hat{\sigma}_k^x)$, $\hat{Z}_{2\gamma_p}^{(2)} = \exp(i\gamma_p \hat{\sigma}_k^z \hat{\sigma}_m^z)$, $\hat{Z}_{2\gamma_p}^{(3)} = \exp(i\gamma_p \hat{\sigma}_k^z \hat{\sigma}_m^z \hat{\sigma}_n^z)$, $\hat{Z}_{2\gamma_p}^{(4)} = \exp(i\gamma_p \hat{\sigma}_k^z \hat{\sigma}_m^z \hat{\sigma}_n^z \hat{\sigma}_l^z)$. (d) Fidelity of finding the right solution as function of the number of layers for the PUBO and QUBO algorithms, followed by (e) the behavior of the cost function for each model.

outperform the standard approach. While fidelity measurements should be avoided in QAOA algorithms, we also show the fidelity in this case as an additional metric of the performance of the circuits. But, the relevant result for QAOA is shown in 1e, where we present the cost function behavior in function of the number of layers.

3.2. Factorizing higher numbers

Going beyond the few digit numbers factorization we use the standard and QUBO approach to factorize all numbers shown in [Appendix A](#), Table A1. For all cases, we repeat the procedure aforementioned using the cost function as main quantity to guide the classical optimizers of our QAOA protocols. To provide a robust characterization of the performance of each protocol, we first investigate the number of CNOTs per layer, in Fig. 2a, and the (absolute) lowest values achieved for the cost function \mathcal{C}_{\min} for different factorized numbers N , shown in Fig. 2b.

As the main conclusion, the scaling advantage of the *QUBO factorization* over the standard formulation is clearly demonstrated—at least, to the cases considered here. The presence of three- and four-body interaction terms in the PUBO Hamiltonian introduces a noticeable degradation in the performance of the PUBO-QAOA, while the QUBO formulation requires substantially fewer CNOT gates per layer. Consequently, even in cases where both approaches efficiently identify the correct factors (for instance, when $N \leq 77$), the QUBO digitized factorization achieves this with a significantly lower gate count per layer. Moreover, the most remarkable outcome of this work arises when considering larger numbers such as $N = 119$ and 143 , each requiring eight qubits. In these cases, the QUBO algorithm exhibits a clear advantage in efficiency and reliability

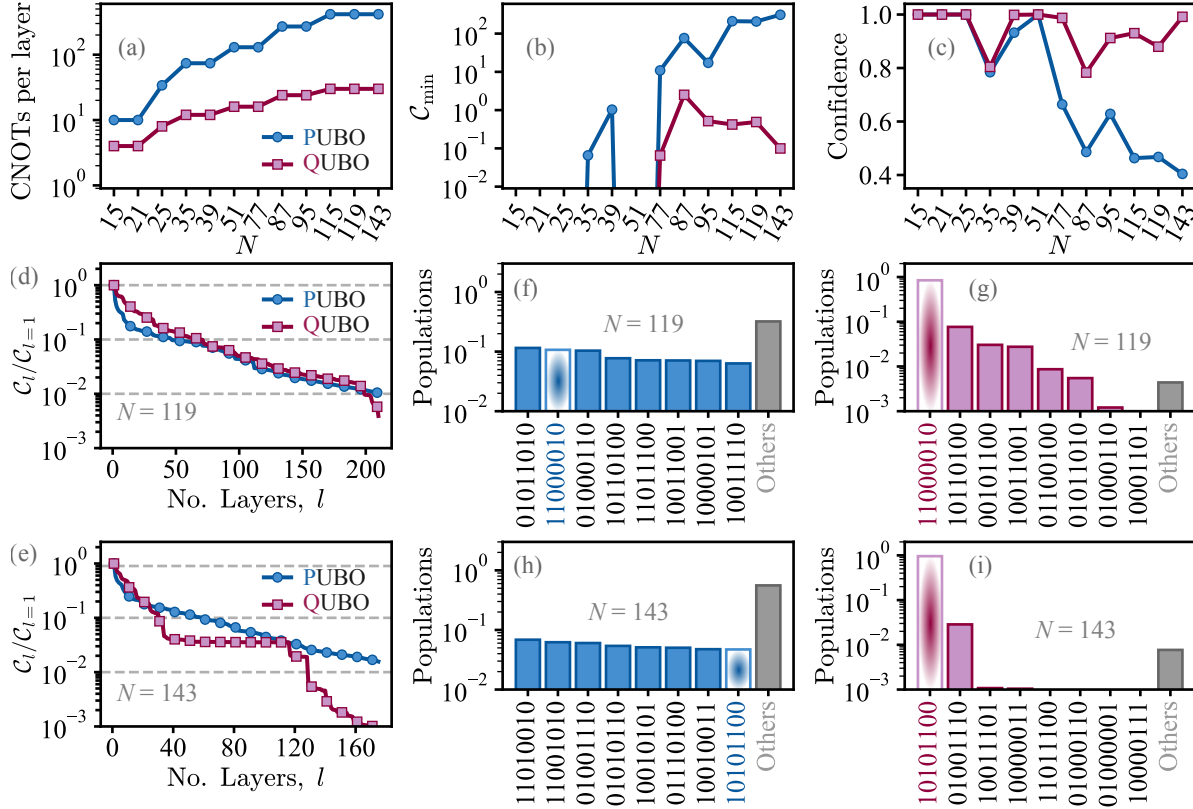


Figure 2. (a) Single-layer circuit scaling of PUBO and QUBO algorithms in terms of the number of CNOTs per layer as a function of N . In (b) and (c), respectively, we show the behavior of the smallest (final) value of the cost function C_{\min} and the confidence of each algorithm as function of N . For the number $N = 119$ we present (d) the normalized cost C_l/C_{l-1} as function l , showing the behavior of the cost for each algorithm. Complementarily, we show in (f) and (g) the population distribution in the computational basis ordered from highest to lowest populated states for the PUBO and QUBO algorithms, respectively, where we highlight the corresponding desired solution. Similar data are shown for the number $N = 143$ in (e,h,i). “Others” constitutes the sum of populations of all computation states not displayed.

for identifying the correct solution, outperforming the standard PUBO formulation for adiabatic factorization.

A key feature of adiabatic quantum algorithms lies in their ability to amplify the probability amplitudes of states corresponding to valid or near-valid solutions, such as search-based algorithms. The overall success of the algorithm therefore depends on its capacity to populate these promising states with high probability. For this reason, an important performance metric is the *confidence* of the output state—that is, the probability weight associated with the correct or near-correct solutions. To quantify this confidence, we measure the overall uncertainty of the distribution using *Shannon entropy*, $H = -\sum_i p_i \log(p_i)$, given the normalized amplitudes (in our case populations) p_i of all states. Because a low entropy value indicates that the distribution is sharply peaked, it suggests that one outcome strongly dominates and thus the prediction

is highly confident. Conversely, a high entropy implies that several outcomes have comparable amplitudes, which corresponds to a higher level of uncertainty. To obtain a normalized confidence score, one can define

$$C = 1 - \frac{H}{H_{\max}}, \quad (6)$$

where H_{\max} is the entropy of a uniform distribution over all possible outcomes. In other words, we compute it using the input state, or we can use directly that in this case we have $p_i = 1/2^n$, where n is the number of qubits in the system. This yields a confidence measure $C \in [0, 1]$, where $C = 1$ corresponds to maximum confidence and $C = 0$ to complete uncertainty.

This significant enhancement in the confidence is confirmed by the monotonically decreasing behavior of the cost function, and the distribution of probabilities of the output state from each protocol, as shown in Fig. 2. As we can see from Figs. 2d and 2e, the *normalized* cost functions for factorization of the highest factorized numbers, namely 119 and 143, behave as expected during the QAOA implementation. By normalizing the cost function by the single layer cost function $\mathcal{C}_{l=1}$, we observe that the QAOA circuit for the QUBO Hamiltonian can reduce the initial energy by up to 3 orders of magnitude (for $N = 143$), while the standard model is able to reduce the cost function up to 2 order of magnitude. In particular, the factorization of $N = 143$ clearly shows the emergence of a barren plateaus [33] for the QUBO Hamiltonian. Even under this undesirable scenario, it is remarkable that the QUBO performs better than its PUBO counterpart.

Complementarily, we identify the solution prime numbers, q' and p' , by reading the final populations distributions in the computational bases in Figs. 2f-2i, sorted from the most populated states, with the accumulated population “Others” representing all other states. As we can see, the good confidence of the QUBO approach is most due to high population transfer to given state, that can be tested as solution of the problem. As indicated by the confidence parameter, in Fig. 2c, the distribution of probabilities for both number is flattened, leading to a uncertainty of the right solution. Most drastically, by testing all states we can identify the solution and, in both cases, they are not placed as most populated states.

3.3. Hamiltonian spectral density analysis

To explain the enhanced performance of the QUBO algorithm, we conjecture that QAOA is mainly impacted by (i) the convergence of optimization—due to local minima trapping [10, 34] or barren plateaus [33, 35], for instance—and (ii) probability of escape from the ideal solution and adiabatic passage [36, 37]—as digitized adiabatic algorithms are also affected by the adiabatic minimum gap condition [38]. Regarding (ii), we can state that for a fixed minimum gap, the higher the density of accessible states, the higher the probability that the quasi-adiabatic QAOA evolution drives the system away from the target computational subspace. For this reason, we investigate the spectral

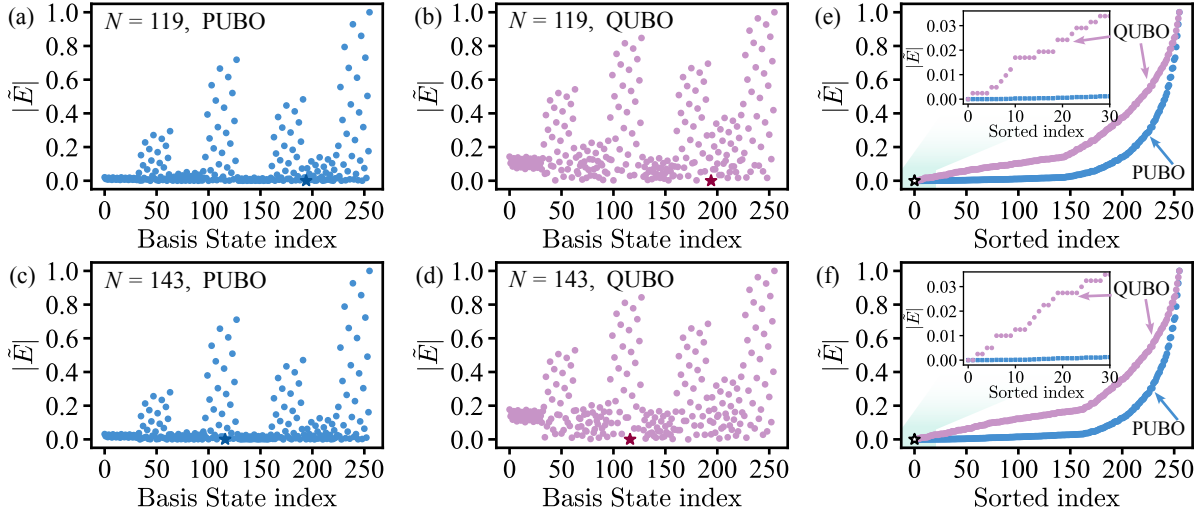


Figure 3. Normalized energy spectra $|\tilde{E}_n| = |E_n|/E_{\max}$ of the (a) PUBO Hamiltonian and (b) QUBO Hamiltonian used for factorization of $N = 119$, where the x -axis shows the decimal encoding of computational basis states. The eigenstate corresponding to the solution ($\tilde{E} = 0$) is marked with red star symbol. Similar plots are shown for the number $N = 143$ in (c) and (d). The panels (e) and (f) show the same spectra as (a,b) and (c,d), respectively, but we use a basis ordering based on the energy $|\tilde{E}_n|$. This graphs, including the inset plots, allow us to observe how the minimum norm $|\tilde{E}_n|$ search is challenged by the high density of states in the PUBO algorithm compared to the QUBO approach.

decomposition of the problem QUBO and PUBO Hamiltonians, where we observe that the density of states of the PUBO Hamiltonian, around the solution subspace, is much higher than its QUBO counterpart.

In Fig. 3 we show the scatter plot of the normalized eigenenergies $\tilde{E}_n = E_n/E_{\max}$, where E_{\max} is the highest eigenenergy, of the problem Hamiltonians as function of the basis state index. From the results shown in Figs. 3a–d, it is possible to understand the reason why the QUBO Hamiltonian provides enhanced results in comparison with its PUBO counterpart. It is evident the high density of states with energy near to the ground state of the PUBO Hamiltonian, while the QUBO spectrum is much less dense around the eigenenergy $\tilde{E} = 0$.

The impact of high density spectrum of the PUBO Hamiltonian becomes even more evident when we consider the ordering of the eigenenergies, as shown in Figs. 3e and 3f, and their inset plots. We find that the spectrum of \hat{H}_{LP} is more widely spread around the solution, leading to larger separations between relevant energy levels near to the kernel subspace. However, it presents multiple degenerate states, which might be related to the emergence of the barren plateaus shown in Fig. 2e. On the other hand, the flattened spectrum of the PUBO Hamiltonian around low-energy states also extends to higher energy states. This constitutes a relevant barrier to classical optimizers in supporting an efficient redistribution of amplitude during the variational evolution. Eventually, this may be the main reason behind the population distribution profile shown in Figs 2f

and 2h.

4. Conclusion

In this paper, we introduced an efficient digitized algorithm for implementing adiabatic factorization, with enhanced success fidelity and circuit complexity. The first major outcome of our study is that the circuit-level enhancement achieved through our approach holds pivotal importance for experimental implementations of digitized quantum computing, as it leads to a substantial reduction in the total algorithmic runtime. Moreover, across all cases analyzed, our QAOA implementation based on the QUBO Hamiltonian consistently yields the correct factorization result, characterized by a highly populated target state that ensures strong confidence in the outcome. In contrast, the same strategy fails to achieve comparable performance when employing the PUBO Hamiltonian for factorization. Consequently, our findings shed new light on the ongoing discussion regarding the relative performance of PUBO versus QUBO formulations in QAOA-based optimization, as our results stand in clear contrast to previous reports in the literature [39].

The most relevant difference between our QUBO proposal for adiabatic factorization and its PUBO formulation is the encoding of the solution in a state in the middle of the Hamiltonian spectrum, rather than in the ground state. While this represents a challenge for quantum annealers—since the ground-state protection against decoherence cannot be exploited [40, 41]—it does not pose a problem for digitized quantum annealers, where decoherence is instead governed by local single-qubit decay. In this scenario, the QUBO approach is expected to be more robust than the PUBO one, as QUBO requires significantly fewer gates per block, thereby reducing the total runtime of the algorithm. Moreover, this reduced gate demand is also expected to constitute an advantage of QUBO-based factorization over its PUBO counterpart in any realistic setting with finite gate error rates.

Looking ahead, our results motivate further exploration of digitized adiabatic protocols in broader optimization and number-theoretic settings. In particular, extending our framework to larger composite numbers and more complex problem Hamiltonians may offer deeper insights into the practical advantages of QUBO-based implementations. Moreover, studying the interplay between circuit depth, noise resilience, and Hamiltonian structure could guide the development of more resource-efficient quantum algorithms tailored for near-term devices.

Data availability statement

The data and codes that support the findings of this study will be openly available in Zenodo following an embargo at the following URL: <https://zenodo.org/records/18414560>.

Conflict of interest

The authors declare no competing interests.

Funding

JJGR acknowledges support from the EuroHPC Joint Undertaking under project QEC4QEA (Ref. 101194322), and by project PCI2025-163266 funded by MICIU/AEI/10.13039/501100011033. ACS is supported by the Comunidad de Madrid through the program Ayudas de Atracción de Talento Investigador “César Nombela”, under Grant No. 2024-T1/COM-31530 (Project SWiQL).

Author contributions

All authors have contributed equally to this work.

ORCID iDs

Felip Pellicer  <https://orcid.org/0009-0002-3686-5586>

Juan José García-Ripoll  <https://orcid.org/0000-0001-8993-4624>

Alan C. Santos  <https://orcid.org/0000-0002-6989-7958>

References

- [1] Peng X, Liao Z, Xu N, Qin G, Zhou X, Suter D and Du J 2008 *Physical Review Letters* **101** 220405
- [2] Barends R, Shabani A, Lamata L, Kelly J, Mezzacapo A, Heras U L, Babbush R, Fowler A G, Campbell B, Chen Y, Chen Z, Chiaro B, Dunsworth A, Jeffrey E, Lucero E, Megrant A, Mutus J Y, Neeley M, Neill C, O’Malley P J J, Quintana C, Roushan P, Sank D, Vainsencher A, Wenner J, White T C, Solano E, Neven H and Martinis J M 2016 *Nature* **534** 222
- [3] Farhi E, Goldstone J, Gutmann S and Sipser M 2000 *arXiv e-prints* quant-ph/0001106 (*Preprint quant-ph/0001106*)
- [4] Farhi E, Goldstone J, Gutmann S, Lapan J, Lundgren A and Preda D 2001 *Science* **292** 472–475
- [5] Shor P 1996 Fault-tolerant quantum computation *Proceedings of 37th Conference on Foundations of Computer Science* pp 56–65
- [6] Barends R, Kelly J, Megrant A, Veitia A, Sank D, Jeffrey E, White T C, Mutus J, Fowler A G, Campbell B, Chen Y, Chen Z, Chiaro B, Dunsworth A, Neill C, O’Malley P, Roushan P, Vainsencher A, Wenner J, Korotkov A N, Cleland A N and Martinis J M 2014 *Nature* **508** 500–503
- [7] Terhal B M 2015 *Rev. Mod. Phys.* **87**(2) 307–346
- [8] Nielsen M A and Chuang I L 2011 *Quantum Computation and Quantum Information: 10th Anniversary Edition* 10th ed (New York, NY, USA: Cambridge University Press) ISBN 1107002176, 9781107002173
- [9] McClean J R, Romero J, Babbush R and Aspuru-Guzik A 2016 *New Journal of Physics* **18** 023023
- [10] Cerezo M, Arrasmith A, Babbush R, Benjamin S C, Endo S, Fujii K, McClean J R, Mitarai K, Yuan X, Cincio L and Coles P J 2021 *Nature Reviews Physics* **3** 625–644
- [11] Farhi E, Goldstone J and Gutmann S 2014 A Quantum Approximate Optimization Algorithm (*Preprint 1411.4028*)

- [12] Peruzzo A, McClean J, Shadbolt P, Yung M H, Zhou X Q, Love P J, Aspuru-Guzik A and O'brien J L 2014 *Nature communications* **5** 4213
- [13] Zhou L, Wang S T, Choi S, Pichler H and Lukin M D 2020 *Phys. Rev. X* **10**(2) 021067
- [14] Bharti K, Cervera-Lierta A, Kyaw T H, Haug T, Alperin-Lea S, Anand A, Degroote M, Heimonen H, Kottmann J S, Menke T, Mok W K, Sim S, Kwek L C and Aspuru-Guzik A 2022 *Rev. Mod. Phys.* **94**(1) 015004
- [15] Larkin J, Jonsson M, Justice D and Guerreschi G G 2022 *Quantum Science and Technology* **7** 045014
- [16] Zhou Z, Du Y, Tian X and Tao D 2023 *Phys. Rev. Appl.* **19**(2) 024027
- [17] Zhang Z, Paredes R, Sundar B, Quiroga D, Kyriolidis A, Duenas-Osorio L, Pagano G and Hazzard K R A 2024 *Quantum Science and Technology* **10** 015022
- [18] Lin J, Zhang Z, Zhang J and Li X 2022 *Phys. Rev. A* **105**(6) 062455
- [19] Ozaeta A, van Dam W and McMahon P L 2022 *Quantum Science and Technology* **7** 045036
- [20] Tabares C, Muñoz de las Heras A, Tagliacozzo L, Porras D and González-Tudela A 2023 *Phys. Rev. Lett.* **131**(7) 073602
- [21] Tabares C, Kokail C, Zoller P, González-Cuadra D and González-Tudela A 2025 *PRX Quantum* **6**(3) 030356
- [22] Tabares C, Wild D S, Cirac J I, Zoller P, González-Tudela A and González-Cuadra D 2025 *arXiv e-prints* arXiv:2511.04434 (*Preprint* [2511.04434](https://arxiv.org/abs/2511.04434))
- [23] Hu C K, Xie G, Poulsen K, Zhou Y, Chu J, Liu C, Zhou R, Yuan H, Shen Y, Liu S, Zinner N T, Tan D, Santos A C and Yu D 2025 *Nature Communications* **16** 3289
- [24] Anschuetz E R, Olson J P, Aspuru-Guzik A and Cao Y 2018 Variational Quantum Factoring *arXiv:1808.08927* [quant-ph]
- [25] Hegade N N, Paul K, Albarrán-Arriagada F, Chen X and Solano E 2021 *Physical Review A* **104** L050403
- [26] Hegade N N, Chen X and Solano E 2022 *Phys. Rev. Res.* **4**(4) L042030
- [27] Chermoshentsev D A, Malyshev A O, Esencan M, Tiunov E S, Mendoza D, Aspuru-Guzik A, Fedorov A K and Lvovsky A I 2021 *arXiv e-prints* arXiv:2106.13167
- [28] Nagies S, Geier K T, Akram J, Bantounas D, Johanning M and Hauke P 2025 *Quantum Science and Technology* **10** 035008
- [29] Babbush R, O'Gorman B and Aspuru-Guzik A 2013 *Annalen der Physik* **525** 877–888
- [30] Albash T and Lidar D A 2018 *Reviews of Modern Physics* **90** 015002 ISSN 0034-6861, 1539-0756
- [31] Harrigan M P, Sung K J, Neeley M, Satzinger K J, Arute F, Arya K, Atalaya J, Bardin J C, Barends R, Boixo S, Broughton M, Buckley B B, Buell D A, Burkett B, Bushnell N, Chen Y, Chen Z, Ben Chiaro, Collins R, Courtney W, Demura S, Dunsworth A, Eppens D, Fowler A, Foxen B, Gidney C, Giustina M, Graff R, Habegger S, Ho A, Hong S, Huang T, Ioffe L B, Isakov S V, Jeffrey E, Jiang Z, Jones C, Kafri D, Kechedzhi K, Kelly J, Kim S, Klimov P V, Korotkov A N, Kostritsa F, Landhuis D, Laptev P, Lindmark M, Leib M, Martin O, Martinis J M, McClean J R, McEwen M, Megrant A, Mi X, Mohseni M, Mruczkiewicz W, Mutus J, Naaman O, Neill C, Neukart F, Niu M Y, O'Brien T E, O'Gorman B, Ostby E, Petukhov A, Puterman H, Quintana C, Roushan P, Rubin N C, Sank D, Skolik A, Smelyanskiy V, Strain D, Streif M, Szalay M, Vainsencher A, White T, Yao Z J, Yeh P, Zalcman A, Zhou L, Neven H, Bacon D, Lucero E, Farhi E and Babbush R 2021 *Nature Physics* **17** 332–336
- [32] See complete data and analysis in Python notebooks for this work from Felip Pellicer's [repository](#).
- [33] McClean J R, Boixo S, Smelyanskiy V N, Babbush R and Neven H 2018 *Nature Communications* **9** 4812
- [34] Lyngfelt I and García-Álvarez L 2025 *Phys. Rev. A* **111**(2) 022418
- [35] Arrasmith A, Holmes Z, Cerezo M and Coles P J 2022 *Quantum Science and Technology* **7** 045015
- [36] Sarandy M S, Wu L A and Lidar D A 2004 *Quantum Information Processing* **3** 331–349
- [37] Amin M H S 2009 *Phys. Rev. Lett.* **102**(22) 220401
- [38] Santos A C 2025 *Phys. Rev. A* **111**(2) 022618

[39] Stein J, Chamanian F, Zorn M, Nüßlein J, Zielinski S, Kölle M and Linnhoff-Popien C 2023 Evidence that pubo outperforms qubo when solving continuous optimization problems with the qaoa *Proceedings of the Companion Conference on Genetic and Evolutionary Computation* GECCO '23 Companion (New York, NY, USA: Association for Computing Machinery) p 2254–2262 ISBN 9798400701207

[40] Albash T, Boixo S, Lidar D A and Zanardi P 2012 *New Journal of Physics* **14** 123016

[41] Albash T and Lidar D A 2015 *Phys. Rev. A* **91** 062320

Appendix A. Table of factorized numbers

The details about all numbers factorized in our work are shown in Table A1 below.

Table A1. Overview of all semiprime instances considered in this work, including the number of qubits n required for the QAOA, the values of p , p' , q and q' , the binary number representation for p' and q' , as well as the expected outcome $|\psi_{\text{out}}\rangle$ in the computational basis.

N	n	p (p')	q (q')	n_p	n_q	$p_{\text{bitstring}}$	$q_{\text{bitstring}}$	$ \psi_{\text{out}}\rangle$
15	3	3 (1)	5 (2)	1	2	1	10	$ \psi_{\text{out}}\rangle$
21	3	3 (1)	7 (3)	1	2	1	11	$ \psi_{\text{out}}\rangle$
25	4	5 (2)	5 (2)	2	2	10	10	$ \psi_{\text{out}}\rangle$
35	5	5 (2)	7 (3)	2	3	10	011	$ \psi_{\text{out}}\rangle$, $ \psi_{\text{out}}\rangle$
39	5	3 (1)	13 (6)	2	3	01	110	$ \psi_{\text{out}}\rangle$
51	6	3 (1)	17 (8)	2	4	01	1000	$ \psi_{\text{out}}\rangle$
77	6	7 (3)	11 (5)	2	4	11	0101	$ \psi_{\text{out}}\rangle$
87	7	3 (1)	29 (14)	3	4	001	1110	$ \psi_{\text{out}}\rangle$
95	7	5 (2)	19 (9)	3	4	010	1001	$ \psi_{\text{out}}\rangle$
115	8	5 (2)	23 (11)	3	5	010	01011	$ \psi_{\text{out}}\rangle$
119	8	7 (3)	17 (8)	3	5	011	01000	$ \psi_{\text{out}}\rangle$
143	8	11 (5)	13 (6)	3	5	101	00110	$ \psi_{\text{out}}\rangle$, $ \psi_{\text{out}}\rangle$